PROCEEDINGS

14th INTERNATIONAL CONGRESS ON ACOUSTICS

14e CONGRÈS INTERNATIONAL D'ACOUSTIQUE

14. INTERNATIONALER KONGRESS FÜR AKUSTIK

VOLUME/BAND 2

C, D, E

BEIJING, CHINA

3 – 10 SEPTEMBER 1992

A PIEZOELECTRIC BONE HYDROPHONE FOR MEDICAL ULTRASOUND APPLICATIONS

V.R. Singh, Sanjay Yadav and Aftab Ahmed

National Physical Laboratory
New Delhi-110012(India)

ABSTRACT

Bone has been investigated as a piezoelectric material for long time now. This piezoelectric property of bone has been utilized to develop a hydrophone. Small pieces of bone, invitro, are cut and shaped to circular form with pencil type tip which is coated with conductive silver point. This bone element is the sensing element of the hydrophone. Electrical leads are connected for excitation and the hydrophone is tested for its frequency response, etc. The hydrophone developed is useful in the study of the field patterns of an ultrasound source.

INTRODUCTION

Piezoelectricity in bone was first investigated by Fukada and Yasuda (1). The temperature and hydration dependence of piezoelectric, elastic and dielectric constants of bone was then reported by the same group (2). Studies were made to understand the mechanism of bone growth, fracture healing and bone remodelling by authors (3-6). A piezoelectric bone transducer element was then developed using the piezoelectric properties of bone (7). Presently, the ceramic type transducers are used as active ultrasonic devices due to their high piezoelectric and electromechanical coupling coefficients but some of the disadvantages were observed when using in biological specimens due to mismatching between the transducer ceramic material element and a biological medium. In this Laboratory, piezoelectric transducer elements from bone were made (7) which were found with lower dielectric and acoustic impedance than those of ceramic type transducer. A piezoelectric bone hydrophone is developed for quantitative measurements of the ultrasonic field of medical ultrasonic transducers. Design and development and results are reported here.

DESIGN AND FABRICATION

A photograph of the bone type hydrophone thus developed is shown in Fig. 1. A small piece of bone was cut from the middiaphysis of bone and shaped to the form of a cone with the based of 2 to 4 mm in diameter. Conducting air dry silver paste was used on the base and the tip surfaces to make conductive for taking electrical connections. This is the sensing element of the hydrophone which was then mounted in a perspex made hollow pipe for both mechanical support as well as acoustic coupling.

In order to achieve adequate spatial resolution and good directional characteristics, the diameter of base surface was reduced to 2-2.5 mm.

The present bone hydrophone was characterised for its frequency response, etc., and calibration by measuring the output voltage in an ultrasonic field of known intensity. The frequency response of bone hydraphone is shown in Fig. 2 over a frequency range of 1-30MHz. Two peaks of maximum output at 5.4 MHz and 17.5 MHz were found. These may be due to the fundamental frequency and its higher harmonies Due to the wide frequency band, it is hoped that use of such bone type hydrophone will enable us to study the nonlinear phenomena at higher frequencies (10 MHz) for ultrasound propagation in different biological media. A systematic study was also made on plotting of beam of an ultrasonic source. A pattern obtained on CRO at 3 MHz frequency is shown in Fig. 3. As the frequency increases above 10 MHz the measurement procedure becomes more difficult due to stray electric fields and high precision manipulation is required. As in the present study there was no preamplifier used, the cable length plays critical role in affecting the response of the transducer an such frequencies. The cable length was, however comparable on eighth of a wave length (8). The sensitivity of the proble was critically controlled by the impedance of the element in relation to length of the cable used as reported in the past (8-9).

CONCLUSION

A piezoelectric bone hydrophone has been developed. The frequency response of the hydrophone is discussed over the frequency range of 1 MHz-30 MHz.

REFERENCES

1. E. Fukada and I. Yasuda, "On the piezoelectric effect of bone", J. Phys. Soc. Jpn., Vol. 12 pp 1158-1162, 1957.

2. H. Maeda, K. Tsuda and E. Fukada, "The dependence on temperature and hydration of piezoelectric dielectric and elastic constants of bone", Jpn. Appl. Phys., Vol. 15, No. 12, pp 2333-2336, 1976.

3. V.R. Singh and Sanjay Yadav, "Earlier hearing of bone fracture with compressive loading: An acoustic investigation", Applied Acoustics, Vol. 25, pp 295-300, 1988.

4. V.R. Singh, V.N. Bindal, V.P. Adya, Sanjay Yadav and Aftab Ahmead, "Non-invasive diagnosis of bone fracture healing", Presented at First AFSUMB Congress, Tokyo, Japan, 1987 (Full Paper in Proc.) (In Press).

5. V.R. Singh, V.P. Adya, Aftab Ahmed and Sanjay Yadav, "A stress wave propagation technique for bone repair study", Submitted to IEEE Trans. on Biomed. Eng., 1987.

6. Sanjay Yadav and V.R. Singh, "Determination of national frequency of bone: Study of bone abnormalities", J. Acoust. Soc. Am. Suppl., Vol3 3, 523, 1988.

7. V.R. Singh, Aftab Ahmed and Sanjay Yadav, "Electrical and mechanical properties of bone", J. Institution of Engineers (India), 1988 (In Press).

8. P.A. Lewin, "Miniature piezoelectric polymer ultrasonic hydrophone probes", Ultrasonics, Vol.19, pp 213-216, 1981.

9. J.R. Bacon, "Characteristics of a PVDF membrane hydrophone for use in the range 1-100 MHz", IEEE Trans. Sonics Ultrasonics, Vol. SU-29, No. 1, pp 18-25, 1982.

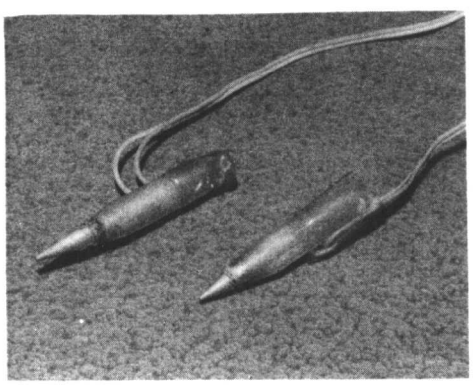

Fig. 1 PHOTOGRAPH OF THE PIEZOELECTRIC BONE HYDRO PHONE

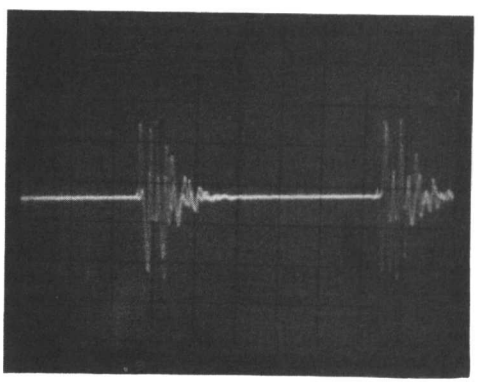

Fig. 3 RESPONSE OF BONE HYDROPHONE UNDER ULTRASONIC FIELD OF 3 MHz TRANSDUCER

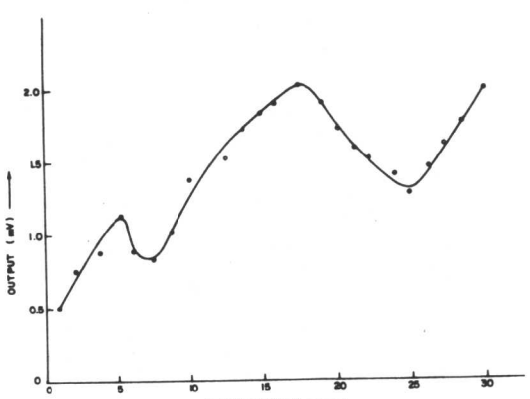

Fig. 2. FREQUENCY RESPONSE OF BONE HYDROPHONE.

Physical Optimization of Focused Ultrasound Surgery.

C. R. HILL, G. R. ter HAAR, R. L. CLARKE, and I. RIVENS

Joint Department of Physics, Institute of Cancer Research, Royal Marsden Hospital, Sutton, Surrey, SM2 5PT, UK.

Previous theoretical models of the formation of thermally mediated ultrasonic focal lesions in tissue have been based on empirical equations designed specifically to fit particular authors' focussing systems (1,2). To a good approximation however, if side-lobe structure is temporarily ignored, focal beam profiles, both axially and laterally, are Gaussian. This allows ready development of a more general and flexible model. We require to solve, in two-dimensional, cylindrically symetrical form, for a Gaussian distribution of thermal input, the transient bioheat transfer equation (3):

$$- \alpha\nabla^2 T + w\sigma(T-T_A) + \rho\sigma\, \partial T/\partial t = Q_m + Q_p \quad (1)$$

where T is the local temperature of the tissue; T_A is the ambient temperature (taken, for perfused tissues, as that of arterial blood); w is the blood perfusion (kg m^{-3} s^{-1}); Q_m and Q_p are the local metabolic rate and ultrasonic power deposition rate (wm^{-3}). Also necessary for the following discussions are the tissue properties: density, ρ; specific heat, σ; thermal diffusivity, α; and ultrasonic intensity absorption coefficient μ and attenuation coefficient η.

In the present context the metabolic term is insignificant and if, initially, we also ignore the perfusion and thermal diffusion terms, focal beam exposure will lead to a temperature distribution indicated in Fig. 1, and a corresponding lesion diameter d (=2x) given by:

$$\Delta T = (T_T - T_A)\, \exp(d^2/0.72D^2) \quad (2)$$

where D is the 6dB beam width, and $\Delta T = T - T_A$.

For a tissue exposed at a penetration depth ℓ to an *in situ* intensity $I_\ell = I \exp(\eta.\ell)$:

$$\Delta T = (\mu I t/\rho\sigma)\, \exp(-\eta.\ell) \quad (3)$$

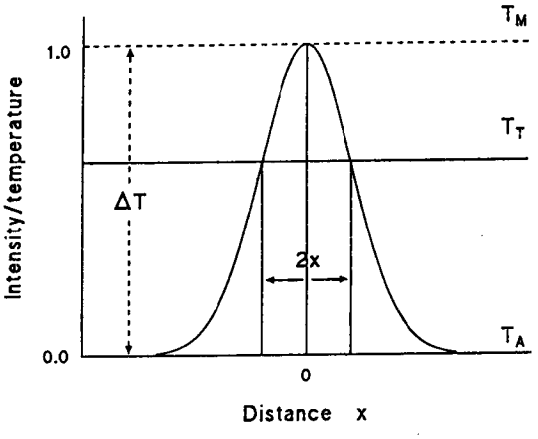

Figure 1: Temperature distribution resulting from exposure to a gaussian beam of tissue at an ambient temperature T_A.

The effect of perfusion is conventionally modelled as removal of heat, at a rate proportional to local temperature elevation, from all tissue elements, thus reducing temperature elevation by a time dependent factor:

$$F_p(t) = \exp(-wt/\rho) \quad (4)$$

In the present case in particular gaussian shape and width parameter value are retained and eq.(3) is modified as:

$$\Delta_p T = F_p(t)(\mu I t/\rho\sigma)\, \exp(-\eta.\ell) = F_p(t).\Delta T \quad (5)$$

The effect of the thermal diffusivity term in Eq.1 has been investigated by Filipczynski and Wojcik (4) who find a corresponding fractional reduction in the peak temperature attained after an exposure of duration t:

$$F_d(t) = K \ln(1+K^{-1}), \text{ where } K = D^2/5.56\,\alpha t. \quad (6)$$

Since however (in the absence of perfusion) thermally deposited energy is conserved and, as shown by the same authors, Gaussian shape is retained following thermal diffusion, the corresponding fractional change in width of the thermal source distribution will be $F_d(t)^{-\frac{1}{2}}$.

The effects of perfusion and diffusion are assumed to be independent and multiplicative and we therefore have:

$$\Delta T.F_p(t).F_d(t) = (T_T - T_A)\, \exp[d^2/0.72(D.F_d(t)^{-\frac{1}{2}})^2] \quad (7)$$

From which:

$$d^2 = 0.72D^2/F_d(t).[\ell n\Delta T - \ell n(T_T - T_A) + \ell n F_p(t) + \ell n\, F_d(t)] \quad (8)$$

Here d is the diameter of the lateral temperature profile, at the level $(T_T - T_A)$, achieved on completion of an exposure of duration t. It can readily be shown that, if power is switched off at this point (i.e. I = 0), d will always thereafter decrease again in value.

Eq.8 is a general predictor of focused lesion diameter and can also be used to derive, from experimental data, a value for the hypothetical threshold temperature, T_T, and to investigate any dependence of T_T on exposure duration. It is based however on a number of simplifying assumptions, and experimentally observed departures from its predictions may be expected on a number of grounds, including the following:

(a) Thermal "lesioning" is presumably a physico-chemical process, quite possibly related to protein denaturation, which is likely to be exposure time dependent (5).

(b) At the peak intensities necessary for lesioning (typically 1-10kW cm^{-2}) finite amplitude ("non-linear") propagation behaviour arises (6), with consequent anomalies in absorption coefficient.

(c) Also, at these intensities, cavitation may play a substantial role in causing increase and inhomogeneity in heat deposition (7).

(d) The Gaussian approximation to beam shape used here generally appears to be good for the central part of the beam that is directly responsible for thermal lesioning and its quantitative inaccurracy seems likely, in practice, to be overshadowed by the preceding factors. The model will be inappropriate, however, for predicting the consequence of one lesioning exposure in raising the effective ambient temperature, T_A, in a closely adjacent site for a subsequent lesion.

One particular value of the model arises from the fact that well documented lesion size data are considerably more abundant and readily obtained for excised than for living, perfused tissues, and it will probably always be necessary to make some use of the former data base and the above theoretical structure in extrapolating to *in vivo* human and animal situations.

REFERENCES

(1) Robinson, T. C.; Lele, P. P. (1972) An analysis of lesion development in the brain and in plastics by high-intensity focused ultrasound at low megahertz frequencies. J.Acoust.Soc.Amer. 51, 1333-1351.

(2) Lizzi, F.L.; Ostromogilski, M. (1987) Analytical modelling of ultrasonically induced tissue heating. Ultrasound in Med. Biol. 13, 607-618.

(3) Billard, B. E., Hynynen, K., Roemer, R. B. (1990) Effects of physical parameters on high temperature ultrasound hyperthermia. Ultrasound in Med. & Biol. 16, 409-420.

(4) Filipczynski, L., Wojcik, J. (1991) Estimation of transient temperature elevation in lithotripsy and in ultrasonography. Ultrasound in Med. & Biol. 17, 715-721.

(5) Carstensen, E.L.; Miller, M.W.; Linke, C.A. (1974) Biological effects of ultrasound. J. Biol. Phys. 2, 173-192.

(6) Swindell, W. (1985) A theoretical study of non-linear effects with focused ultrasound in tissues: an "acoustic Bragg peak". Ultrasound in Med. & Biol. 11, 121-130.

(7) Lele, P. P. (1986) Effects of ultrasound on "solid" mammalian tissues and tumours *in vivo*, in "Ultrasound: Medical Applications, Biological Effects and Hazard Potential". (Ed. Repacholi, M.H.; Grondolfo, M.; Rindi, A) New York, Plenum.

ENHANCED ENZYMATIC ACTIVITIES IN MOUSE TISSUES FOLLOWING IN VIVO EXPOSURE TO ULTRASOUND

R.P.Surendra Kumar

Department of Zoology
S.K.University
Anantapur 515 003, India.

Ultrasound interaction with biological tissues is adequately reported. The diagnostic as well as the therapeutic applications have been well explained to the finer details. Most of the earlier workers were mainly concentrating on the modality, physical parameters and, to some extent on the impact on the histopathological status of the tissues. However, the effect of this non-ionizing radiation at sub-cellular level is still in a nascent stage. Over the last 8 years we have been involved in investigating the effects of ultrasound on various pathological and normal tissues, specially studying the enzyme activities following irradiation. Mouse model has been taken up for experimentation. A wide range of enzymes like Dehydrogenases, ATPases, Synthases, Phosphorylases, Amylases, in mouse liver and pancreas and Acetylcholinesterases and associated neurotransmitter were estimated in foetal liver and brain following the exposure to in vivo and in utero to a fixed period of ultrasound. Besides, silk worm (Bombax mori) eggs at 12 h stage were irradiated to find out the effect of ultrasound on the enzymatic system of early embryonic development.

Swiss-Webster mice were used for experimentation after acclimatizing them to the laboratory, and giving the food and water ad-libitum. A 12 h photocycle was maintained. Healthy adult mice of both sexes were anesthetized with pentathol sodium (120 u g/g body weight) and the ventral abdomen surface was shaved and cleansed with a mild detergent. Acoustic coupling jelly was smeared on to the cleansed surface and the transducer with 2.5 cm radiating aperture was clamped tightly on the skin over the liver region. Six day old pregnant mice were exposed in utero by placing the transducer over the right horn of the uterus. Silk worm eggs were irradiated in a glass beaker in a degassed water medium. The in vivo experiments were done with the transducer directly coupled to the skin avoiding the aqueous coupling medium which was hitherto followed by earlier workers. Ample care was taken to eliminate the formation of standing waves by using rubber padded boardes beneath the mice and glass beakers. Continuous wave of unfocussed ultrasound of 875KHz was driven from the signal generator supplied by Ralsonics India. Batches of 10 animals were exposed to 5, 10 and 15 W/cm^2 for a period of time ranging from 60s to 90s per fraction. The irradiation was repeated for 5 days with an exact gap of 24 h between two successive exposures. Thus a total exposure of 300 and 450s was spread over five days. The silk worm eggs were treated for 240s only at one sitting.

Animals were sacrificed on day zero, day one, day five and day 10 following the last exposure of the regime and target tissues were excised immediately to proceed for the enzymatic estimations. Enzyme study was done as per the standard procedures (Govindappa & Swami, 1965; Nachalas et al., 1966; NIN, 1983; Yeung, 1968; Joseph & Subramanyam, 1972; Sutherland, 1955; Le Loir & Goldsmith, 1960, Tobine et al., 1979, Augistinson, 1957; Metcalf, 1957; and Otsuka et al., 1971).

More than 50 samples were taken for assay for each parameter. The enzymes recorded a significant increase throughout the experimentation and in all the exposed organs. Table 1 shows the enhancement of enzymes in all the groups of samples. The minimum and the maximum ranges of elevation in each enzyme and amongst all the exposure and sacrifice levels are presented in the table. Except for a few cases where the level of enzymes was not significantly altered, the elevation was found significantly increased in all the enzymes.

Previous reports on the ultrasonic effects were mainly histopathological or gross changes (O' Brien et al.,1978; Kumar and Raju, 1989; Stolzenberg et al., 1983). Very few have reported the changes at sub cellular level (Edmonds and Sancier, 1983; Rosenfield et al., 1984; Kaufman , 1985; Kondo,1985; Crum, 1987; Haga et al., 1987; Ma et al., 1987; and Suneetha and Kumar, 1991).

The present experimentation reveals that ultrasound is capable of enhancing the cellular secretions, although these secretion, whether enzymes or others have a certain impact on the cellular physiology of the tissue in question. The enhancement of enzymes and neurotransmitters keeps the foetal brain in a state of stress, which if allowed to continue, may enter a comatous condition. This is further evidenced by the depletion of oxygen in the exposed foetal brain tissues. When pancreas was exposed, the significant raise in the ATPases and, the increase in fructose-1-6 phophatase, glycogen phophorylase, glycogen synthase, and other ATPases in liver as a sympathetic reaction of the pancreatic irradiation, show that there in an enhanced activity in the release of insulin along with the changes in cell membrane permeability. This is important since it could help in diabetic research. Further, the increase in the lengths of the silk fibres is again a resultant of enzyme

enhancement. Ultrasound appears to have made a profound impact on the early embryonic development, may be at the early transcription, which needs further investigations. Also induced is, the early entrance of the larva into the spinning which saves the farmer one full feed which is economically viable. This paper is humble attempt to put forth that ultrasound can be tried to enhance the cellular secretions.

Table 1.

Enzyme	Enhancement %	
	Min	Max
Adult Liver		
SDH	03	66
MDH	25	77
LDH	19	50
FDPase	04	116
G-phosphorylase	08	118
G-synthase	07	180
Total ATPase	03	50
Na-K-ATPase	10	37
Mg-ATPase	02	15
Adult Pancreas		
Total ATPase	10	45
Na-K-ATPase	15	56
Ca-ATPase	02	42
Mg-ATPAse	05	17
Alpha-Amylase	00	17
Foetal Liver		
SDH	38	129
MDH	48	68
LDH	50	87
Foetal Brain		
SDH	172	262
MDH	101	130
LDH	130	210
ACh	54	74
AChE	73	80
GABA	56	78
Silk Fibre		
Length	7.0mt	7.5mt

SDH - Succinate dehydrogenase
MDH - Malate dehydrogenase
LDH - Lactate dehydrogenase
FDPase - Fructose-1-6-diphosphatase
G-phosphorylase - Glycogen phosphorylase
G-syntahse - Glycogen synthase

References

Augistison,K.N.B. Methods of Biochemical analysis,(1957) 15, Wiley, New York

Crum, L.A. Walton, J.J. Mortimer, A. Dyson, M. Crawford, D.C. and Gaitan, D.F. J Ultrasound in Med and Biol (1987) 6, 643-647

Edmonds, P.D. and Sancier, K.M. Ultrasound in Med and Biol (1983) 6, 635-639

Govindappa,s. and Swami,K.S. Ind J exp Biol (1965) 3(4) 209-212

Haga, M. Shimura,T. Nakamura, T. Kato, Y. and Suziki, Y. Chem Pharm Bull (1987) 35, 3822-3830

Joseph,P.K. and Subramanyam,K. Biochem J (1972) 128, 1298

Kondo,T. and Yoshi, G. Ultrasound in Med and Biol (1985)11, 113-119

Kaufmann, G.E. Ultrasound in Med and Biol (19985) 11, 497-501

Le Loir, L.F. and Goldenberg, S.H. J Biol Chem (1960) 235, 919

Ma, C. Kenzic,P.I. and Mosser, M. Comp Biochem Physiol (1976) 54 B, 103-106

Metcalf, R.L. Methods of Biochemical analysis (1957) 5, Inter Science Publication Inc. New York

Nachalas, M.M., Margulieam S.L. and Seligman, A.M. J Biol Chem (1960) 235, 499-503

NIN (National Institute of Nutrition Indian council of Medical Research Manual of Laboratory Techniques (1983) 190

O'Brien,W.D. Brady, J.K. and Dun, F. J Ultrasound in Med and Biol (1978) 5, 35-43

Otusuka, M. Obata, K. Miyata, Y.and Tanaka, Y. J Neurochemistry (1971) 18, 287-295

Stolzenberg, S.J. Torbit, C.A. Edmonds, P.D. and Taenzer, J.C. Radiat environ Biophys (1983) 17, 245-270

Suneetha, N.and Surendra Kumar, R.P. Ultrasonics (1991) 29, 257-260

Surendra Kumar, R.P. and Sebastian Raju, G Ind J Exp Biol(1989) 27, 23-25

Sutherland, E.W..Methods in Enzylology I(1955) 215-225, Academic Press, New York

Tobine,R.W. Berdanier, C.D.and Ecklund, R.E. J Environ Pathol Toxical (1979) 2. 1247

Yeung, D. Stanley, R.R. and Oliver, I. Biochem J (1968) 105, 1219

COMPUTER-BASED AUTOMATED ULTRASONIC INTERFEROMETER FOR BIOMEDICAL APPLICATIONS

G. M. SRINIVASAN and B. KANICKAIRAJ

Department of Physics, St Joseph's College, Tiruchirapalli 620 002, India

1. INTRODUCTION

The use of the ultrasonic investigations is becoming more and more acceptable and reliable not only in the study of liquids and solutions but also in industrial and medical applications. The need and desirability of "Automation" of the ultrasonic techniques with a view to enhancing the speed and other capabilities is evident. The ultrasonic interferometer is one of the powerful instruments frequently used as it can be used with considerable ease and accuracy.

In this background the set objectives of our work reported in this paper are:

i) To completely mechanise the operations of the ultrasonic interferometer appropriately using a stepper motor.
ii) To recognise, digitaly, the presence/crossing a node/antinode of the standing wave pattern set up in the liquid medium between the transducer and the reflector of the interferometer.
iii) To develope computer program to (a) start (b) count the number of steps and (c) stop the operation at the end of prescribed number of logic '1' states.
iv) To design and fabricate the peripherals needed for the work.
v) To write finally the program for the mathematical calculations and display/print the result.

2. EXPERIMENTAL SET UP

The block diagram of the automated ultrasonic interferometer is presented in Fig. 1.

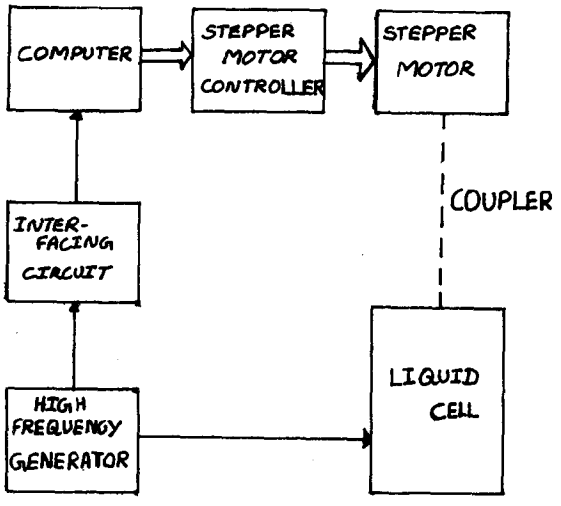

FIG.1. BLOCK DIAGRAM OF THE COMPUTER BASED AUTOMATED ULTRASONIC INTERFEROMETER

2 MHz oscillations from the generator transferred to the liquid in the cell through a quartz crystal sets up mechanical oscillations. A reflector fixed to the tip of a micrometer screw arrangement can be moved up and down by working the screw. The ultrasonic waves propagated in the liquid medium travel back and forth in the liquid. If the separation between the reflector and the crystal is exactly a whole multiple of sound wavelength, standing waves are formed in the medium, resulting in acoustic resonance with the formation of nodes and antinodes. The reflected waves reaching the crystal cause variations in the anode current of the oscillator circuit. The currentmeter reflects these variations in the conventional interferometer and thus provides a method of locating the nodes and antinodes. If the micrometer screw is worked continuously, the reflector moves through the successive nodes and antinodes, thus causing a sinusoidal current variation. The distance between the successive nodes, and hence the half wavelength of the waves in the medium can be measured with the help of the micrometer scale.

As the first step of the mechanisation the operation of the micrometer screw-head is done using a stepper motor. The way in which the assembly is realised is shown in Fig. 2.

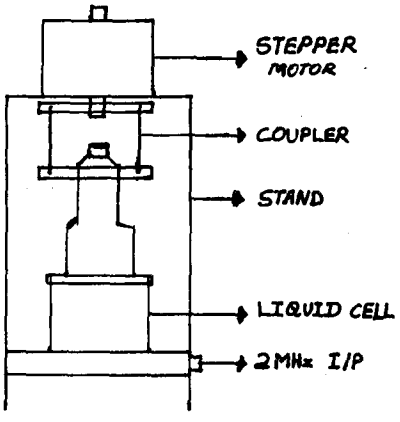

FIG.2. FOUR-PILLERED ASSEMBLY

It consists of a four-pillered stand that houses the measuring cell on a platform at the bottom and the stepper motor at the top. The shaft of the motor is connected to the micrometer screw head through a coupler arrangement. The advantage of using a stepper motor is that the computer can keep track of exactly where the plunger is at any given time. The computer is used to control the functions of the stepper motor. Figure 1 shows the block diagram of the computer controlled stepper motor. The main activities of control involve starting the motor, stopping the motor after counting 20 maxima and effect the forward or reverse motion of the plunger. The appropriate software for such operations is discussed in Section 4.

3. INTERFACING TECHNIQUE

The sinusoidal current variations between the successive nodes and the antinodes of the standing waves as reflected in the oscillator circuit is suitably converted as voltage variation across a resistor. The analogue voltage variations are converted to the corresponding digital values with the help of the interfacing circuit shown in Fig. 3.

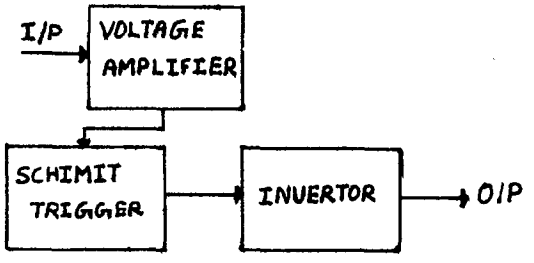

FIG. 3. BLOCK DIAGRAM OF THE INTERFACING CIRCUIT.

The 'automation' of the interferometer achieved is such that the ultrasonic velocity gets directly recorded and displayed/printed. This step requires (i) recording the distance moved for 20 "Hi" levels and (ii) all the related mathematical calculations, besides starting the stepper motor "ON" and controlling its motion.

The procedure adopted is: For one complete rotation of the head of the micrometer screw the reflector moves a distance equal to the pitch of the micrometer screw (0.5 mm) and an angular displacement of 360°. When one sequence is given to the stepper motor, the motor rotates 1 step, say, clockwise. The arrangement is that the motor makes 200 steps to complete one rotation. Thus for 1 step of rotation the shaft will make 1.8° rotation and the corresponding distance moved by the reflector is 0.0025 mm.

Thus the computer is enabled to check the maxima within 0.0025 mm of reflector movement. Thus a high resolution is achieved. To calculate the distance moved by the reflector between two maxima: we note that if 'S' be the number of sequences between two maxima viz. for half wavelength, the ultrasonic velocity in metres per second is S/2.

Thus half the number of sequences for 20 maxima gives the velocity of ultrasound in the given liquid.

4. COMPUTER PROGRAM

With this background the flowchart for developing the computer program for achieving the result is given. (see next column).

5. BIOMEDICAL APPLICATIONS

Ultrasound is widely used as a routine clinical diagnostic, therapeutic and surgical applications in different parts of the body. It has provided us an important and widely accepted method for non-invasive imaging of the human body that offers great potential

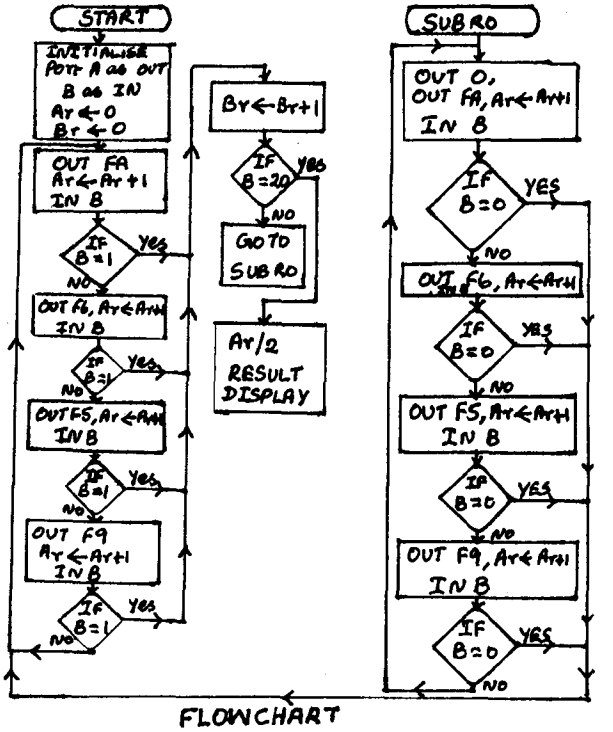

FLOWCHART

for further development in diagnostic medicine, the reason being that ultrasound energy has the ability to propagate through soft biological tissues suffering only moderate attenuation. The ultrasonic propagation properties of tissues are governed to some extent by their biochemical composition. Thus the characterisation of the tissues and biomaterials is possible by determination of the wave propagation parameters such as velocity and attenuation of ultrasonic waves.

The automated ultrasonic interferometer developed is a first step towards the study of biological fluids leading to their characterisation. the work on automation of attenuation measurements and the multiple frequency ultrasonic interferometer are in progress.

REFERENCES

Blitz, Jack, **Fundamentals of Ultrasonics** (Butterworths, London, 1967).

Gooberman, G. L., **Ultrasonics: Theory and Applications** (The English University Press, London, 1968).

Malvino, **Digital Electronics** (McGraw-Hill, New York, 1977).

Millman, Jacob, **Microelectronics** (McGraw-Hill, New York, 1979).

Rajaraman, **Programming in Basic** (Prentice-Hall of India, New Delhi, 1988).

Sheingold, Daniel H, ed., **Analog Digital Conversion Handbook** (Analog Devices Inc., USA, 1972).

C1-6

ULTRASONIC STUDIES IN LIQUID BIOLOGICAL SYSTEMS

Anil Suryavanshi and V.R. Singh
National Physical Laboratory
New Delhi-110 012 INDIA.

ABSTRACT

Biological materials liquid or solid have been investigated for adulteration due to its adverse effect on human beings. An ultrasonic double-probe-through-transmission technique has been developed and used to detect adulteration in biological and biologically significant materials, mainly liquids in the present study. The technique has been found to provide quite reliable results and has an advantage of no energy loss due to reflection or adsorption etc. The liquid materials studied here are some adulterated food systems and diesel which can have adverse biological effects.

INTRODUCTION

Liquid and solid biological materials if used in adulterated form can result in severe health hazards. Whenever, medical drugs alcohol and blood infusion have any and of unwanted contamination, it may be fatal to the user or patient. Not only humans even machines and heavy vehicles get affected by using adulterated fuels. Cheaper quality kerosene oil is frequently used as an adulterant with petrol which in turn librate lot of hazardous smoke and spoil the environment by polluting it.

In order to detect adulteration in materials of biological importance a study has been undertaken. Food systems are mainly inhomogeneous in nature (1), while some of them are porous, the others are emulsive. Generally fruit items are seedy in natural form and have complex and layered structure. Oily items are, kerosene, mostly homogeneous and solid fats have properties similar to those of biological tissues. Spices, vegetables and cheese etc. are also porous in nature.

Processed milk cream and vegetable oils are among the materials studied for the adulteration detections. The constituents of edible oils and fats are, relatively simple aliphatic compounds. Oils and fats are mostly triglycerides (2) which are esters of glycerol with fatty acids. In nature, fatty acids comprise of glyceride molecules. Vegetable oils and facts are artifically processed by hydrogenation for making products. Falty acids are in the form of straight chain and even numbered showing acetic (CH_3CO_2H), butyrix ($C_3H_7\ CO_2H$) molecules.

Processed milk cream and vegetable oils when mixed appear to be similar. In fact fat contents in both are almost the same. When processed milk cream with vegetable oil is heated above their melting points, they turn into a transparent yellowish liquid. To detect this new composition, ultrasonic technique is quite useful in such studies as the absorption and velocity of ultrasound depend upon the concentration of fat.

Another food system studied is honey mixed with sugar. Honey is, of two types, one form obtained through extraction and other form squeezing from bees behives. Properties of both of these are almost the same. Pure natural honey if used in adulterated form with products like sugar, glucose, etc. for medical purposes, would have ill effect or no effect on treatment. Sugar is used as an adulterant in the honey for laboratory work.

Diesel and kerosene oil are also studied for their ill effects on environment (3). A double probe-through-transmission technique is developed for the study of all the above stated systems. Ultrasonic velocity and isentropic compressibility are then calculated which are related to the percentage of adulteration.

THEORY

Ultrasonic velocity (V) is determined by using the following formula ,

$$V = d/t \quad \ldots\ldots\ldots(1)$$

where 'd' is the distance between the receiving and the transmitting transducer and 't' is the time taken by the ultrasonic waves to travel the distance 'd'.

Compressibility (β) is theoretically defined as follows:

$$\beta = 1/v^2\rho \quad \ldots\ldots\ldots(2)$$

where 'ρ' is the density of the sample used. Intermolecular distance (L) can also be determined, if required, by using the formulae,

$$L = T/\sqrt{\beta} \quad \ldots\ldots\ldots(3)$$

where 'T' is a temperature dependent factor.

EXPERIMENTAL DETAILS

The experimental set up used in the present investigation for the detection of adulteration using ultrasound is shown in Fig.1.A glass tube of 6.5 cm in length and the internal diameter 30 mm with two openings opposite to each other accommodating two ultrasonic transducers of 2.5 MHz was used. The transducers were kept fixd in the water proof rubber corks in the openings. The face to face distance between the two matched transducers was 4.5 cm which could be changed by changing the position of the transducer accordingly. A syringe needle was used to fill up the liquid chamber for testing. On the other side an additional tube was used to let the air go out. It is important to make sure that there was no air bubble inside,which otherwise affects the calibration of the system. A pulser-receiver (parametics, Model 5052 PR) was used to excite the transmitting transducer as well as receiving transducer. Ultrasonic waves travelling through the sample under test were amplified and displayed on CRO screen after being received by the receiving transducer.

Samples or mixture of different liquid systems to be studied were prepared in different ratios, upto 1:1. The sample under test was put into the sample holder and the time taken (4) by the ultrasonic wave to travel from transmitter to the receiver in the liquid medium was monitoredwith the help of calibrated CRO screen. The ultrasonic velocity and insentropic compressibility were then calculatd.

RESULTS AND DISCUSSIONS

The results obtained on different ratios of adulteration in different systems are shown in Table I, II and III. The velocity (V) and compressibility (β) are plotted (Fig 2, 3, and 4) for different percentages of adulteration from 1 to 100%. In diesel and kerosene, ultrasonic velocity is found to decrease with the increase in adulteration of kerosene.

Honey is found to retain its flavour and taste upto 50% of mixing of sugar. So, it is generally difficult to predict about adulteration on the basis of flavour or taste, though honey is denser than the sugar in liquid solution. The velocity of ultrasound is found to increase with the increase in the quantity of honey and hence the percentage of sugar is found to decrease. Isentropic compressibility is inversely proportional to the square of the ultrasonic velocity. Both velocity and compressibility can be used to detect the percentage of adulteration after proper calibration. Temperature is also a factor on which the ultrasonic velocity and thus the percentage of adulteration depends. Temperature maintained during the experiment was 30.5 C.

The attenuation of ultrasound in a fatty medium is the resultant intrinsic attenuation of various components. This also depends upon the scattering (ε), viscosity and thermal properties of the media. Fat components which are dispersed in the form of globules, are the main cause of thermal losses. The velocity is found to be more dependent on the fat contents of these items. In the present study ultrasonic velocity is found to decrease as the quantity of adulterant (vegetable oil) is increased.

Ultrasonic double probe technique has also been proved to be very useful for the study of various properties of food systems. Earlier the study of binary liquid mixtures (7-9) and measurement of moisture (10) have been done by using a vertical path ultrasonic interferometer technique, but this is found unreliable for adulteration in oils, because it has a problem of calibration and is thus time consuming.

In the ultrasonic testing of fruit juice, percentage of fruit flesh or sugar contents are determined. Wine (11), milk and emulsions are studied for the knowledge of the quality of fat and oils. Crispnes of biscuits crack detection of cheese, thickness of egg shells, moisture content of ice cream, smoothness of orange sking and cracks of tomato skin are also studied and analysed.

CONCLUSION

Detection of adulteration in different systems have been performed using double probe-through-transmission technique. The technique on comparison is found better than other ones specially the single probe method. A portable instrument has also been designed taking into consideration the above results for the investigation of adulteration in liquid and solid materials.

REFERENCES

1) Javanau , C., Application of ultrasound in the food systems, ultrasonics, 1982, Vol. 26, May, pp.117-123.

2) Hampson, G.C. and Hudson, J.F.,Physical and Chemical properties of the constituent of edible oils and fats, proc. of a conference arranged by Unilever Limited at Research Department Port Sunlight, March 10-12, 1959, pp.1-19.

3) Kumar, A.,Singh, V.R. and Parashar D.C. Ultrasonic Detection of Adulteration in Diesel, Jour;nal of Research and Industry,India, Sep.1991. pp.168-170.

4) Mak, D.K., Somerville, I.R. and Kung, W., Automatic Measurement of Travel Time in Ultrasonic Inspection, Journal of NDT, 31, Jan. 1983, page-13.

5) Allegra, J.R. and Haily, S.A., Attenuation of Ultrasound in suspensions and emulsions, theory and experiments, J.Acoust,soc.Am.51,1972,pp.1545-1563.

6) Miles, C.A., Shere, D. and Larglay, K. R., Altenuation of ultrasou in milks and creams, ultrsonics, Nov.1990, Vol. 23, pp.394-400.

7) Pande, P., Parakash, O. and Parakash, S., Workshop and Exhibition on ultrasound therapy and ultrasonic measurements, New Delhi, 1983, page-12.

8) Krikhnababu, M. and Rao, R., Workshop and Exhibition on Ultrasound Therapy and Ultrasonic measurements, New Delhi 1983, page-92.

ICA BEIJING 1992

C1-7

ACOUSTIC STRESS WAVE STUDY IN KIDNEY STONES

V.R. Singh, J.P. Lafaut*, R. Agarwal and J.B. Dhawan

National Physical Laboratory, New Delhi - 110012, India

*K.U. Leuven Campus Kortrijk, Interdisciplinary Research Centre, University Campus, B-8500 Kortrijk, Belgium

INTRODUCTION

Kidney stones are complex composites and there is a large variation in their composition due to the presence of various chemical constituents like calcium oxalate, magnesium-ammonium phosphate, uric acid and cystine. Some of other parameters responsible for such variation are age, sex, climate and nature of food habits of the patient. Disintegration of renal calculi, without surgery, is now an important subject of research. One of the disruption methods which is in use, these days, is the use of focussed shock waves. This technique is non-invasive and gives less discomfort to the patients. Physical mechanisms involved in the disruption of kidney stones due to high intense shock wave are, however, not fully understood /1-4/.

The work described in this paper is aimed at investigating the propagation of acoustic stress wave in the kidney stones with regard to the crushing strength required for different types of kidney stones, by using a focussed shock wave lithotripter.

MATERIALS AND METHODS

Kidney stone samples were collected from local hospitals in Delhi, India and were classified according to their chemical constituents determined by pathological means. The crushing strength was found by using a conventional method as reported earlier /1/.

For ultrasonic stress wave study, kidney stone samples were shaped with two opposite flat surfaces parallel to each other /1-3/. A double probe through-transmission technique was used. Stress wave generated by one ultrasonic transducer was allowed to pass through the composite kidney stone sample and was received by another transducer of similar frequency. The whole stress wave was displayed on CRO (cathode-ray-oscilloscope) screen, and was analysed to determine ultrasonic velocity and other parameters.

Focal ultrasound transducer, as used in the disintegration of kidney stones, was utilized to apply pressure on the stone to disrupt its chemical structure and the study of pressure amplitudes was carried out.

RESULTS AND DISCUSSION

When acoustic stress wave from a lithotripter, say ESWL (extracorporeal shock wave lithotripter), is applied to the kidney stone during the treatment, acoustic pressure generated at the surface of the stone which then might disrupt the stone as the pressure wave tries to travel into the stone itself (in compressive mode) from particle to particle and the structure of the stone, in turn, is disrupted. However, some tensile force of kidney stone tries to oppose or resist and hence the actual stress amplitude does not travel further into the stone. But there is second pulse of stress wave and then third and so on, having higher intensity strength than those (tensile) from the stone itself. Thus, the stone particles are disturbed, may be, first from the portion where the stress wave enters into the stone and then subsequently other particles are disturbed which are in the path of the wave and, also due to particle-by-particle propagation of stress wave.

On the other hand, some stress wave is reflected back, in addition to frequency dependent attenuation, and dispersion etc. However, resultant pressures, developed in the lithotripsy fields, are very high and hence, in turn, the stone is broken. Another important factor is that the peak pressures in the acoustic pulses generated by lithotripters cause small shifts in the relative phase of harmonics generated during the propagation of stress wave due to non-linear effects and hence care is required to be taken into the design of such instruments (lithotripters).

With the application of impact load due to focussed shock wave from the lithotripter, the stone sample starts cracking. Strains are developed inside the stone samples, but when the yield point is reached, the stone starts breaking and at the breaking point, it is completely disrupted. By looking at the experimental curve between the crushing load and the strain (see Fig. 3 in Ref. 1), it is clear that this behaves like other solid materials which have similar stress/strain curves. Ultrasonic stress wave parameters (at 2.5 MHz) are reported in Table 1 with respect to crushing strength of different

types of stones measured experimentally /2-3/.

Stress wave generated by the focussed system is required to be investigated further, both theoretically and experimentally. Also, stress wave propagation may be studied in the kidney stones as reported in case of bones /4/.

Acoustic pressure for a focussed Gaussian beam, and on the surface of kidney stone under the shock wave exposure, may be expressed /5/ as a Fourier series as

$$p = \frac{p_0}{2} \sum_{-\infty}^{+\infty} \varphi_n \exp(jn\tau)$$

where p is the acoustic pressure near to the focal lobe, p_0 is the peak pressure at the aperture, φ_n is the nth coefficient of the Fourier series (φ_0 may represent the dc component of the Fourier series), τ is the retarded non-dimensional time, $\tau = \omega_0 (t-z/c_0)$ and ω_0 is the reference angular frequency with displacement z and velocity c_0. It is fundamental angular frequency in case of periodic signals and the pulse repetition for pulsed signals.

Pressure amplitudes may be measured at different points in the focal volume by using a hydrophone. Also, imaging of strain developments in the kidney stones under focussed ultrasound is required to be studied in detail in future to understand the physics of kidney stone disintegration.

CONCLUSION

Acoustic stress wave propagation study has been made in the kidney stones, both with plane and focussed ultrasound, in relation to the crushing strength and constituents of the stones. Effect of the tensile and compressive waves has been reported on the disintegration mechanisms. Pressure waves generated at the surface and inside the stones have been discussed.

REFERENCES

1. V.R. Singh and R. Agarwal, Journal Lithotripsy and Stone Disease (USA), 2(2), 1990, 117-123.
2. R. Agarwal and V.R. Singh, Ultrasonics 29, 1991, 89-90.
3. V.R. Singh and R. Agarwal, JASA, 85, 1989, 962-963.
4. V.R. Singh, V.P. Adya, A. Ahmed and S. Yadav, IEEE Trans. BME 17 (10), 1990, 1014-17.
5. N.P. Kuznetsov, Sov. Phys. Acoust., 16, 1970, 467-70.

Table 1

Average Ultrasonic Stress Wave Propagation Parameters (at 2.5 MHz) with Respect to Crushing Strength in Kidney Stones

	Kidney Stone Type	Ultrasonic Velocity (m/s)	Crushing Strength (kg/mm²)
1	Calcium-Oxalate Monohydrate	2950	98.5
2	Calcium-Oxalate with Hydroxyl-Apatite	2600	54.2
3	Calcium Monohydrate with Calcium Oxalate Dihydrate	2420	33.5
4	Calcium Oxalate Monohydrate with Uric Acid	2210	25.6
5	Calcium Oxalate Monohydrate with Calcium Oxalate Dihydrate and Hydroxyl-Apatite	2160	22.5
6	Magnesium-Ammonium Phosphate Hexahydrate with Carbonate Apatite	2070	20.4

BEIJING 1992

C1-8

ULTRASONIC CHARACTERIZATION OF BREAST TISSUE

P. D. EDMONDS, C. L. Mortensen, J. S. Ostrem, P. Schattner and L. A. Shifrin

Bioengineering Research Laboratory, SRI International, Menlo Park, California 94025 USA

Ultrasound mammography is the method of choice for differentiating solid from liquid-filled lesions. Ultrasound remains unreliable, however, in the crucial task of distinguishing benign from malignant lesions. A preliminary clinical study [1] using ultrasound computed tomography indicated that computer-aided classification of tissues based on changes in sound speed and attenuation between the suspicious region and surrounding (presumably normal) tissue was diagnostically superior to visual analysis. In the literature the attenuation data for breast tissue display apparent contradictions that are important to resolve in the context of transmission imaging and computed tomographic reconstruction. Some authors [2-3] working with tissue specimens fixed in formalin have associated high attenuation with malignancy, moderate attenuation with benign disease, and low attenuation with normal breast tissue; fixation had no effect on these results. In contrast [4], deductions from ultrasonic CT imaging data indicate that the attenuation of malignant, benign, and normal breast tissue in vivo spans the same range. Thus, it is important to collect a body of reliable data that is extensive enough to enable ultrasound attenuation and speed to be characterized in terms of detailed pathological changes.

METHODS

The approach selected to measure both attenuation coefficients and sound speeds in breast tissue is the substitution technique, comparing tissue specimens with reference solids and liquids having known ultrasound properties. Measurements of insertion loss are made with 4-microsecond bursts at 1-MHz intervals in the range 2 to 9 MHz and best fitting curves of frequency dependence are obtained. Sound speed is derived from time of flight of a pulse, effectively at a frequency of 6 MHz. A detailed report of measurement methods has been published [5].

RESULTS AND DISCUSSION

We have previously reported results of analysis of 118 sets of data for sound speed and attenuation coefficients as functions of frequency in the range 3 to 8 MHz, derived from measurements at 37 C on freshly excised breast tissue [6]. The data comprised 47 sets for normal tissue, 55 for abnormal but benign, and 16 for malignant tumors. Each data set consisted of the attenuation coefficients at 5 and 8 MHz, the intercept and slope of attenuation as a function of frequency, the sound speed, and the patient's age. By using a neural network, which was trained on a random selection of 75% of the data sets, we were able to classify the remaining 25% of the data sets in the three categories of interest: normal tissue, abnormal but benign, and malignant tumors [7]. The network was a fully-connected, feed-forward configuration with 6 inputs (the variables), 2 hidden layers of 12 and 9 nodes, and 3 outputs (the categories). It was trained by using a back-propagation algorithm [8], which adjusted the network weights to minimize the mean-square classification error. After training, all the data in the training sets were classified correctly (Table 1). The results for the test set of 31 cases are shown in parentheses in Table 1. All four malignant tumors were classified correctly. One out if 12 cases of normal tissue was misclassified as a benign lesion, and 4 out 15 benign lesions were misclassified as normal tissue. The classification performance of this neural network was considerably superior to that resulting from using discriminant analysis and superior to that resulting from using classification trees [6].

Table 1. Neural net classification results: numbers of cases in 75% training set (25% test set). Model: In 6-12-9-3 Out; 1501 iterations. Error rate (number of cases misclassified/total number of cases) = 4.2%

	True Class		
Predicted Class	Benign	Malignant	Normal
Benign	40(11)	0(0)	0(1)
Malignant	0(0)	12(4)	0(0)
Normal	0(4)	0(0)	35(11)

To obtain a visual impression of the way the data sets can be clustered in the three different categories, we also made use of a Kohenen self-organizing network [9], which employed an unsupervised learning algorithm. The 6 input nodes, to which the feature values were applied, were fully connected to a 2-dimensional array (25 x 25) of output nodes. The data sets were presented to the network and the initially small, randomized weight values of the internodal connections were adjusted according to the learning algorithm. After this training was completed, we presented each of the data samples again and labelled the output node that was "turned on". The result was a natural ordering of the data sets in the output plane, such that data samples with like characteristics appeared at output nodes in the same region (Figure 1). Note that the malignant tumor samples cluster near the center, the benign tumor samples tend to cluster near the upper left, although there are numerous exceptions, and the normal tissue samples tend to cluster near the bottom right. As many of the benign lesions were fibroadenoma, the clustering shown in Figure 1 is understandable as protraying the significance of a fibrous tissue component and the associated increase of sound speed in the ability to discriminate abnormal from normal tissue. Nevertheless, many data samples for benign lesions "turned on" nodes in the "normal" region, indicating the need for additional input parameters to improve the clustering. Moreover, substantial overlapping of the "benign" and "malignant" regions portends great difficulty in discriminating these two categories. As clinical treatments differ for the two categories, this distinction is crucial for the utility of tissue characterization by ultrasound.

REFERENCES

1. Schreiman, J. S., J. J. Gisvold, J. F. Greenleaf, and R. C. Bahn (1984): Ultrasound Transmission Computed Tomography of the Breast, Radiology, 150, 523-530.
2. Calderon, C., D. Vilkomerson, R. Mezrich, K. F. Etzold, B. Kingsley, and M. Haskin (1976): Differences in the Attenuation of Ultrasound by Normal, Benign, and Malignant Breast Tissue, J. Clin. Ultrasd., 4, 249-254.
3. McDaniel, C. A. (1977): Ultrasonic Attenuation Measurements on Excised Breast Carcinoma at Frequencies from 6 to 10 MHz, Proc. 1977 IEEE Ultrasonics Symposium, pp. 234-236, IEEE Cat. #77CH1264-1SU.
4. Greenleaf, J. F., and R. C. Bahn (1981): Clinical Imaging with Transmissive Ultrasonic Computerized Tomography, IEEE Trans. Biomed. Engrg., BME-28, 177-185.
5. Arditi, M., P. D. Edmonds, J. F. Jensen, C. L. Mortensen, W. C. Ross, P. Schattner, D. Stephens, and W. Vinzant (1991): Apparatus for Ultrasound Tissue Characterization of Excised Specimens, Ultrasonic Imaging, 13, 280-297.
6. Edmonds, P. D., C. L. Mortensen, J. R. Hill, S. K. Holland, J. F. Jensen, P. Schattner, A. D. Valdes, R. H. Lee, and F. A. Marzoni (1991): Ultrasound Tissue Characterization of Breast Biopsy Specimens, Ultrasonic Imaging, 13, 162-185.
7. Ostrem, J. S., A. D. Valdes and P. D. Edmonds, (1991): Application of Neural Nets to Ultrasound Tissue Characterization, Ultrasonic Imaging, 13, 298-299.
8. Rummelhart, D. E., and G. E. Hinton (1986): Learning Internal Representations, in Parallel Distributed Processors: Vol. 1, Foundations, J. L. McClelland et al., eds., pp. 318-330 (MIT Press, Cambridge, Mass.).
9. Kohenen, T. (1990): Self-Organization and Associative Memory, 3rd edn., pp. 107-120 (Springer Verlag, Berlin).

Figure 1. Self-organization of nodes in a plane by application of the Kohenen algorithm and six features of breast tissue derived from ultrasound measurements.

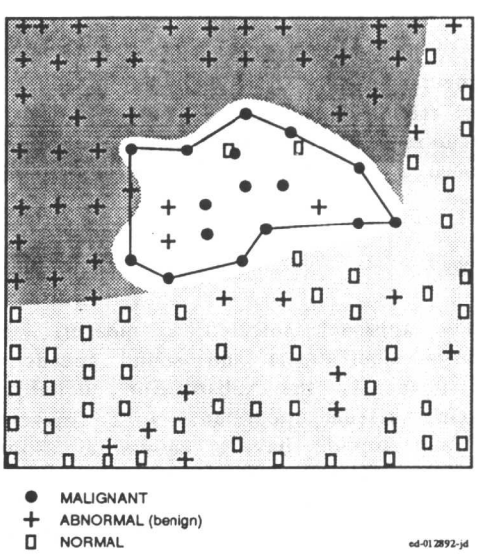

(This research is supported by U.S. PHS Grant CA34398, awarded by the National Cancer Inst.)

C1-9

STUDIES ON CLINICAL TISSUE CHARACTERISATION BY THE WIDTH OF GRAY LEVEL HISTOGRAM

Kazuo MAEDA and Masaji UTSU

Dept. of Obstetrics and Gynecology, Seirei Hamamatsu Hospital, 2-12-12, Sumiyoshicho, Hamamatsu 430 Japan

INTRODUCTION

There have been the reports of basic analysis of radiofrequency ultrasound in the change of its velocity, frequency, attenuation or non-linearity, in ultrasonic tissue characterisation. We have tried frequency dependent attenuation with use of UIP-100 computer system, then the attenation coefficient was obtained in the blood, fetal liver, in-vivo placenta, and uterine fibroids (Akaiwa, 1989). However, the special computer system used in the study was uncommon in clinical laboratories, then the reproducibility was limited in broad meaning.

The other field of tissue characterisation has been the analysis of B-mode image brightness. The technique is the analysis of the video-signal after the processing of reflected ultrasound. The analysis of pixel brightness was started in the evaluation of the gray level of B-mode images. We examined the mean gray levels of gynecological tumors, ovarian changes, and the placenta, then the results showed the usefulness of the width of the gray level. The reproducibility, however, has not been confirmed yet in the width value among ultrasonic imaging devices which prepared the histogram function. Hence, we intended to solve these issues in the present study.

MATERIALS AND METHODS

1.The Gray Level Histogram

B-mode pixel signals stored in the memory of digital scan converter were selected within the region of interest (ROI) which was set at the B-mode image. The number of the pixels counted at every gray scale was normalised by changing it into percentage. The histogram step of the most pixel number was 100% in the ordinate. The abscissa was also normalised to 100% in UIP-100 computer system, but it was still 64 scales in common sonographic devices which prepared the histogram function. The percentage value of histogram width was automatically obtained by UIP-100 computer system, but the percentage was not indicated on the screen of common sonographic devices (Fig.1). Therefore, the histogram width was manually measured on the permanent record of the B-mode screen, and the percentage of the width was calculated dividing the width value by the full gray scale length. Pixel number should be 500 or more, and the histogram peak should be located between 40 to 60% of full gray scale length in this study (Fig. 2).

2. Sonographic Devices in This Study

Many sonographic devices prepared the function of gray level histogram, and we found Aloka SSD-680, SSD-650, Toshiba SSA-270A and Yokogawa R-8000 having the display function of gray level histogram other than Aloka UIP-100 computer system, among the devices which were used in our hospital.

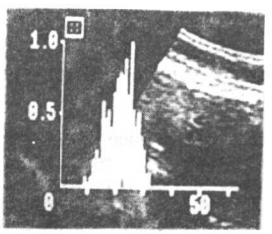

Fig.1.Gray level histogram of a placenta

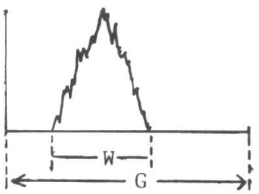

Histogram Width=W/G(%)

Fig.2.Analysis of gray level histogram

3. The Histogram Width of Ultrasonic Phantom in Sonographic Devices

Above described 4 sonographic devices and the computer system were tested with use of RMI 412-A ultrasonic imaging phantom. The homogeneous part of its image was used for the comparison of the histogram width of these devices. The brightness changed, mean gray level varied, and gray level histogram shifted along the histogram abscissa, when the device gain was changed, but the histogram width did not vary by the change of the gain. However, dynamic range or image contrast was related to the width, therefore, the dynamic range was set at large level, or contrast control was set at the lowest scale.

Ultrasound frequency was 3.5 to 3.75 MHz, and convex type transducer was used in the tests. STC, the depth compensation, was off, but later the use of STC was compared to the condition without STC in SSD-680. The use of linear transducer was compared to the convex one in SSD-650. The setting of device control of UIP-100 system was the same as the studies on the placenta and ovarian masses (Kihaile, 1988, 1989). Ultrasonic transducer was placed on the upper surface of the phantom via ultrasonic jelly. The ROI was placed at homogeneous part of the image. The ROI was moved horizontally and vertically on the screen, and the number of ROIs were 8 to 24 in every tested device. The shape of the ROI was square in UIP-100 system, SSD-680, SSD-650,R-8000, and round in SSA-270A. The size of the ROI varied among the sonographic devices.

4.Clinical Studies on the Histogram Width

1)Examination of the Placenta

Normal ranges of the percentage of the width of gray level histogram of the placenta, mean ± 1.5 SD in every two weeks were obtained, by clustering the data of the percentage values of the width obtained by UIP-100 system in 140 to 300 days of pregnancy in the report of Kihaile (1988).

Newly obtained data of the placenta, Grannum grade 0 to III, which was measured placing the ROI at the placenta image after freezing by the use of SSD-680 and SSA-270A, were compared to the normal ranges which were obtained by the above procesing of previous data measured by UIP-100 system.

2)Examination of Fetal Organs

The width values of fetal brain, lung and liver were measured placing the ROIs at the images of these organs by the use of SSD-680 and SSA-270A in middle and late stages of pregnancy.

RESULTS AND DISCUSSION

1.Gray Level Histogram Width of Ultrasound Phantom

There was no significant difference among the percentage values of the width of gray level histogram of RMI 412-A phantom which were obtained by UIP-100 computer system(36.5±4.3%,N=10), SSA-270A (36.1±2.7%, N=14) and SSD-680(36.9±2.3%,N=8) sonographs. The differences among these 3 systems were only 1 % of the value of UIP-100 system, in spite of the arbitarily change of the device gain in order to obtain suitable B-mode image.

SSD-650(32.4±1.3%,N=24) and R-8000(46.0±2.3, N=19) showed significant differences to UIP-100 system, but the differences were as small as 11 and 26 % of UIP-100, hence the devices will be used after the calibration by multiplying small factors.

The depth compensation done by STC of SSD-680 showed no significant influence on the results. The change of transducer from convex to linear showed no change of the values in SSD-650. The ROI shape also had no influence on the results obtained in this study.

However, significant differences of the "Peak(%)" values which represents the mode of gray level or the brightness of the image, were observed, because the device gain was voluntarily changed.

From these results, the width value of gray level hisotgram will be reproducible among the common sonographic devices, whereas the brightness, which is represented by the gray level, will be difficult to reproduce even for the clinical purposes, because the device gain is controled according to the request of the examiner, and also it will be influenced by the depth of the subject tissue.

2.Clinical Examination

1)Examination of the placenta

Newly obtained width values of gray level histogram of the placenta, which were mainly Grannum grade 0 to I, by the use of SSD-680 and SSA-270A, showed the values within the normal ranges which was determined by the processing of previous data obtained by the use of UIP-100 system, whereas Grannum grade III placenta showed the distribution clearly above the upper range of normal placenta.

The results will demonstrate clinical usefulness of the normal ranges of the width of gray level histogram in the assessment of the maturity and pathology of the placenta. As there was significant increase of fetal distress or IUGR in the cases of Grannum grade III placenta (Kihaile,1988), the width of gray level histogram will be valuable in the assessment of fetal wellbeing in high-risk pregnancy.

2)Examination of fetal organs

The widths of the gray level histogram of fetal brain were 29.42±2.68%(N=7) in 24 weeks, 37.14±4.90% (N=6) in 28-29 weeks and 46.10±6.65% (N=11) in 35-36 weeks respectively, and there were significant differences among these values. Fetal lung should be further studied after collection of more data. There was significant difference of the width values of fetal liver between 31.87±2.21%(N=6) in 24 weeks and 39.04±4.23%(N=17) in 35-36 weeks. The results will demonstrate the capability of quantitative tissue character estimation in fetal organs by the use of the width of gray level histogram .

3.Clinical significance of the histogram width

X-ray computed tomography (CT) and magnetic resonance imaging (MRI) prepare the funtion to provide quantitative index or coefficient of their images, and the values strongly influence on physician's decision in clinical diagnosis of the disease. Ultrasound image is superb in the utility at bedside, but it has provided no quantative support for the decision making of medical doctors. Although gray level histogram width value is still empirical but not absolute,we believe medical staffs will use the value as the useful support on the decision making for the diagnosis, then the value will provide the benefit of the patients.

The histogram width represents the difference between the highest brightness and the detectable lowest one of the pixels in a ROI, therefore the width will show the "range" of pixel brightness, hence the width value will be the function of the variance or standard deviation of pixel brightness. As these values are similar to the value obtained by statistical analysis of pixel gray level, we can expect to use more generally acceptable index in clinical tissue characterisation. The method has been already studying in our laboratory, then it will be reported immediately after this paper.

CONCLUSION

The width value of gray level histogram was confirmed to be reproducible among the sonographic devices which prepared the function of gray level histogram by the use of RMI 412-A ultrasound phantom. Normal ranges of the width value were obtained by the procesing of the width values which were reported previously. Newly obtained data of the width of the placenta by the use of other sonographs showed clear discrimination of normal and excessively mature placenta by using the normal ranges of the width value. The width values of fetal organs demonstrated significant differences in the tissues of fetal organs in middle and late stages of pregnancy. There is the possibility further to expand the use of the width in the tissue character estimation in the field of Gynecology, for example, in the assessment of the nature of ovarian masses. Further application of the width value will be found in other medical fields. The width value is still empirical, but it can be changed into more generally acceptable parameter which is in preparation in our study. The ultrasound phantom can be replaced in future study by such natural phantom as the tissue of a normal adult organ.

REFERENCES

1.Akaiwa A; Ultrasonic attenuation character estimated from backscattered radiofrequency signals in Obstetricsand Gynecology. Yonago Acta medica 32:1-10, 1989.

2.Kihaile PE; Ultrasonic grey level histograms of prenatal placenta and its relation to fetal well-being.Yonago Acta medica 31:139-146,1988.

3.Kihaile PE; Ultrasonic tissue characterization of ovarian tumors by the scanning of grey-level histogrms.Yonago Acta medica 32:251-260,1989.